Title: Is the Dynamic Topography signal of the Yellowstone hot spot preserved in the compound topography of the North American plate?

Authors: Eduardo F. Guerrero, Andrew J. Meigs, Patricia M. Gregg

Abstract

The Yellowstone caldera is one surface manifestation of a mantle plume, however, translation of a lithospheric plate over a mantle plume creates dynamic topography that advects through the plate at the rate of plate motion with respect to the mantle. A wave of surface and rock uplift accompanies this advection of dynamic topography. Previous studies of the Yellowstone region have reached two differing conclusions as to whether the plume is expressed topographically. The first is that the high topography (Yellowstone Crescent of High Terrain 'YCHT'), localized seismicity (the 'tectonic parabola'), and a geoid high centered on Yellowstone are thought to represent plume forcing of late Cenozoic tectonics and landscape evolution. The second conclusion is that climate change is the principal driver of landscape evolution in this region. The Yellowstone plume topographic signal, however, is complicated by contributions from plume-related bimodal volcanism, basin and range extension, early Cenozoic arc volcanism, and Laramide contraction to the polygenetic regional topography. In this paper we examine and analyze digital elevation data for the Greater Yellowstone Region to assess the multiple wavelengths of compounded topography to test the existence of long wavelength and low amplitude contribution to elevation from the Yellowstone hot spot.

Introduction

Numerous investigations demonstrate that mantle convective processes such as upwelling affect the surface topography of the overriding plate (Rowley et al., 2013; Flament et al., 2013; Moucha and Forte, 2011; Duller et al., 2012; Burov and Cloetingh, 2009; Saunders et al, 2007; King and Redmond, 2007; Lowry et al., 2000; Wheeler et al., 2000; Gurnis et al, 2000; O'Connell, 1998; Lithgow Bertelloni and Gurnis, 1997; Gurnis, 1990; Hager et al., 1985.). The surface expression of this upwelling has been coined ‘dynamic topography’ (Flament et al, 2013). The earliest development of the dynamic topography concept focused on homogeneous oceanic lithosphere (Von Herzen et al., 1982). Forcing of continental surfaces by mantle processes apparently explains a diverse range of phenomena including drainage reorganization of continent-scale rivers, patterns of uplift and subsidence in mountain belts, and marine inundation of continents (Nereson et al, 2013; Braun et al, 2013; Karlstrom et al, 2012; Peyton et al., 2012; Shephard et al., 2010; Carminati et al., 2009; Wegmann et al., 2007; Saleeby and Foster, 2004). Advection of dynamic topography occurs when lithospheric plates move with respect to the mantle (Braun et al., 2013; Riihimaki et al., 2007; Pierce and Morgan, 1992; Von Herzen et al., 1982; Morgan, 1971). Dynamic topography is thus transient with respect to position in a continent and moves as a wave through continental lithosphere. Whereas orogenic processes create high amplitude (≤ 4 km) and variable (10 – 100’s km) wavelength topography in the continents (Molnar, 1988), low amplitude (<< 1 km) and long wavelength (100 to 1000’s km) characterizes dynamically supported topography (Rowley et al., 2013; Braun, 2010; Lowry et al., 2000). Identification of the surface expression and effects of advecting dynamic topography is thus complicated by inherited topography and the wavelength, amplitude, and transient nature of the mantle forcing on the surface of continental lithosphere (Braun, 2010).

An example of active dynamic topography in the North American plate is thought to result from a mantle thermal anomaly beneath the Yellowstone Volcanic Field, the so-called Yellowstone hotspot (Schmandt and Humphreys, 2012; Smith et al., 2009; Pierce and Morgan, 2009; 1992; King and Redmond, 2007; Humphreys et al., 2000; Lowry et al., 2000) Evidence for dynamic topography associated with the Yellowstone hotspot includes: (1) the highest geoid anomaly (Figure…) in North America corresponds with the Yellowstone region (Lowry et al., 2000); (2) a topographic swell of 400-1000 km in diameter centered on the Yellowstone caldera (Smith et al, 2009); and (3) a parabolic region of high topography/relief and concentrated seismicity that apparently surrounds the caldera (Anders et al., 1989; Pierce and Morgan, 1992; 2009). Deconvolving the signal of dynamic topography associated with the Yellowstone hotspot is complicated by the fact that the volcanic center migrated into a region of crustal thickening and paleotopography (Becker et al, 2013; Lowry et al., 2000), which is revealed by the strong correlation between Laramide structures such as the Beartooth Mountains, the Bighorn Basin, and the Bighorn Range with the detailed structure of the geoid (Figs. 1 and 2). Whereas some authors argue that advection of the dynamic topography has forced the Pliocene to recent landscape evolution of the greater Yellowstone region (Wegmann et al., 2007; Pierce and Morgan, 1992; Anders et al., 1989), models suggest that a well-established switch from subsidence to incision in the Bighorn and other basins thought to be affected by the hotspot is better explained by Pliocene to Recent climate change than by rock uplift associated dynamic topography (Riihimaki and Reiners, 2012; Riihimaki et al., 2007). Thus in spite of the fact that a mantle thermal anomaly underlies the North American plate beneath the Yellowstone region (Smith et al., 2009; Pierce and Morgan, 2009; Saunders et al., 2007; Riihimaki et al., 2007; Humphreys et al., 2000; Lowry et al., 2000), neither the signal of the associated dynamic topography nor the impact on landscape evolution are uniquely identifiable (Nereson et al, 2013; Karlstrom et al., 2012; Wobus et al., 2012; Riihimaki et al., 2007; McMillan et al., 2006)

In this paper, we assess the existence of a topographic swell associated with the Yellowstone hotspot by analyzing digital elevation datasets and relating regional topographic observations to 3-D P wave (V_p) travel-time tomography models for western North America (Schmandt and Humphries, 2010; 2012). First we apply low pass filters to progressively remove shorter wavelength and variable amplitude signals to reveal long wavelength, >400 km topography (Flament et al, 2013). Second, we present swath profiles of the GY/SRP region to identify mean elevation values and analyze the relief structure of the GY/SRP region. Third, we present stream profile analysis results for selected streams draining different areas of the proposed swell. Finally, we parameterize known values for the Yellowstone plume into a model for advection a topographic swell and resulting erosion to better constrain the potential for a geomorphic signature of the hotspot in North America (Braun et al, 2013).

Geologic Setting

Hotspots are generally identified on the earth's surface by linear, age-progressive volcanic centers (Bonatti et al., 1977). Debate within the geophysical community continues as to the origin of mantle hotspots. Early views argued that hotspots represented mantle plumes that rise from mantle anomalies at the Core-Mantle boundary

(Morgan, 1971). More recent studies indicate that mantle plumes form at a variety of depths and that they may follow an upward path dictated by convective processes (Steinberger and O'Connell, 2000).

Whether the Yellowstone hotspot formed due to mantle plume processes is debated as well. One camp argues that crustal processes localize magmatism at Yellowstone (Christiansen et al., 2002). Geophysical data cited by Christiansen et al. suggest that a thermal anomaly beneath the Yellowstone caldera resides near the base of the North American plate and extends no deeper than 200 km. Alternatively, the wealth of geophysical data gathered by Earthscope and modeling results and observations projectdemonstrate that the thermal structure beneath Yellowstone is complex, but that a distinct thermal anomaly exists to depths of 660 – 700 km (Schmandt and Humphreys 2012; Humphreys et al., 2000; Smith et al., 2009). A complex plume thus links the hotspot at surface to depths of ~700 km in the mantle. Regardless of the depth of origin, there is strong evidence to suggest the existence of a mantle upwelling that has contributed to the volcanic, tectonic, and topographic evolution of the Greater Yellowstone region (Refer to Swath profile/p-wave velocities data). V_p at 100 km depth beneath the GY/SRP region indicates that the slowest travel times for these waves is correlated with the position of the Yellowstone Volcanic field, making the transition from Yellowstone to the surrounding areas the largest velocity gradient in Western North America.

The voluminous eruptions of the Columbia River and Steens Mountain flood basalts are considered to be the earliest record of Yellowstone hotspot activity (Parson et al, 1998). An northeastward-younging progression of volcanic centers from eastern Oregon to the Yellowstone caldera constrain the direction and rate of motion of the North American plate with respect to the mantle thermal anomaly (Fig. 1) (Pierce and Morgan, 2009). The first volcanic centers formed at 15 Ma (the McDermitt complex) and then between 13.8 and 12 Ma (the Owyhee-Humboldt complex) (Pierce and Morgan, 1992). Calderas from southwest to northeast distributed along the Snake River Plain include the Bruneau-Jarbridge, which was an active rhyolitic eruptive center from 12.5-11.2 Ma, the Picabo Volcanic Field (PVF; Fig.1) was active between 10.3 and 8 Ma, the Heise volcanic complex (HVF; Fig.1) was active from 6-4 Ma, and finally the Yellowstone

Volcanic Field (YVF; Fig.1) formed after 2 Ma (Pierce and Morgan, 1992). Volcanism at each individual volcanic center lasted approximately 2 Ma. Roughly 150-200 km separates each center. Spacing between the eruptive centers suggests that rate of plate motion with respect to the mantle slowed from 7 cm/yr to 2.9 cm/yr after 10 Ma (Pierce and Morgan, 1992).

The Yellowstone Volcanic Field developed in crust characterized by significant paleotopography as the result of Late Mesozoic – Early Cenozoic Crustal shortening and middle Cenozoic volcanism. Crustal shortening during the Laramide orogeny between 75 and 50 Ma created the Bighorn Basin due to uplift of the Beartooth-Absaroka Mountains on the west, Pryor mountains in the north, Bighorn mountains in the east and Owl Creek mountains in the south (Fig. 1) (Blackstone, 1986). Basement rocks in the core of these ranges mountains are Archean aged (>2.5 Ga) and represent an exposed portion of the Wyoming Craton, an early building block of the North American plate (Hoffman, 1988). Syntectonic alluvial fan deposits preserved along the fringe of the Bighorn Basin suggests that Laramide crustal shortening created topographic relief in excess of 1-2 km between ~73 and 55 Ma (DeCelles et al., 1991; DeCelles and al, 1987). More than 5 km of sediment accumulated in the Bighorn Basin between the early Paleogene and Pliocene (Dickinson et al., 1988). Apatite fission track cooling ages from samples in the Bearooth Mountains range from 61 to 52 Ma document cooling associated with this thrust event (Omar et al., 1994). Track length modeling indicates a second period of cooling started between 15 and 5 Ma and continues to the present. A period of arc magmatism in the Eocene associated with rapid shallow subduction of the Farallon plate followed the Laramide orogeny (Feeley, 2003). The easternmost extent of volcanism is the Absaroka volcanic center, a 55-45 Ma event in the ranges that bound the southwestern edge of the Bighorn Basin (Fig. 1).

Mantle flow explains some geoid anomalies observed at the earth's surface, flow that arises from density contrasts and or temperature anomalies within the mantle (Hager et al., 1985). Long wavelength (>1000 km) variations of the Earth's geoid have been interpreted as the topographic expression of deeper mantle convective processes (Hager et al., 1985; Lithgow-Bertelloni and Silver, 1998). The highest geoid anomaly observed in the continental United States is centered on the Yellowstone Volcanic Field (Fig. 1)

(Smith et al., 2009; Pierce and Morgan, 1992). Geoid anomalies combine the effects of uncompensated high topography as well as zones that are underlain by lower density/hotter material (Hager et al., 1985; Smith et al, 2009). The geoid anomaly centered on Yellowstone is over +12 m higher than the surrounding area, which translates to a positive gravity anomaly of 35 mGals, is thought to reflect the mantle hotspot (Smith et al., 2009).

The series of subaerial volcanic centers represent the primary evidence of the track of the Yellowstone hotspot through the North American plate (Fig. 1) (Christiansen, 2001). A parabolic region of seismicity and active crustal faulting reflects active deformation of the North American plate beyond the limits of the present caldera (Anders et al, 1989). Anders et al (1989) suggest the 'tectonic parabola' region is created as the plate passes over the hotspot. Three nested regions define the parabola: a leading/outer periphery of low seismicity, an intermediate region of concentrated active seismicity, and an aseismic interior (Fig. 2). The Snake River Plain occupies the 'collapse' interior region and defines the axis of symmetry of the parabola. The modern caldera lies on the axis of symmetry within the intermediate, active region of the parabola.

Pierce and Morgan (1992; 2009) were the first to argue that Yellowstone hotspot is expressed topographically. They described the Yellowstone Crescent of High Terrain (YCHT) as being similar to the bow-wave of a ship, a topographic wave where incipient uplift is defined by an area of waxing topography, the apex of uplift in the region of highest topography, and a region of waning topography with subsidence in the wake of the topographic wave (Fig. 2). The YCHT also describes a parabolic region, which although larger in scale, includes Anders et al.'s (1989) tectonic parabola. They attribute the region around the modern caldera and the high relief topography of the Beartooth Mountains to define the axis of the YCHT. On the basis of comparison with oceanic hotspots and on the correspondence between the geoid high and the caldera, Pierce and Morgan maintain that the YCHT resulted from deformation of the North American plate above the mantle plume. Migration of and tilting of streams away from the YCHT in the Bighorn, Yellowstone, and Wind River basins is interpreted to reflect incipient uplift as the hotspot migrated northeastward with respect to North America (Pierce and Morgan, 1992; 2009).

Lowry et al (2000) synthesized elevation data, gravity, crustal-scale seismic refraction, and surface heat flow data in an attempt to isolate the dynamic topography from the region of high elevation centered on the Yellowstone Volcanic Field. Recognizing that the topography reflects the integrated effects of tectonism, volcanism, plate properties, and mantle buoyancy, their model sequentially subtracted the inferred contribution of each variable to arrive at the dynamically supported topography. Model results reveal dynamic topography that is asymmetric in the direction of plate motion, with a gentle SW slope and steep NE slope, has an amplitude approaching 2 km, and has a ~1000 km wavelength (Fig. 2). A curious and unexplained result of their analysis is that the maximum dynamically supported topography is centered on the NE edge of the Snake River Plain to the southwest of the caldera, the YCHT, and the parabola of active seismicity (Fig. 2).

Methods

Digital Elevation Analysis

We performed analyses of 30m Shuttle Radar Topography Mission for the Greater Yellowstone/Snake River Plain (GY/SRP) using ArcGIS 10.21 and Matlab. The purpose of the analyses is to characterize topography at a scale that approximates the wavelength of dynamic mantle processes that underlie the GY/SRP region (Lowry et al, 2000 ; Humphreys et al, 2000; Smith et al, 2009; Schmandt and Humphreys, 2010) that underlie the GY/SRP. We then compare topographic analyses results to geophysical data including upper mantle % deviation of V_p velocity (Schmandt and Humphries, 2010) and geoid anomaly values (EGM, 2008) for the region.

Low-Pass Filters

We applied low pass filters to 30 m void-filled Shuttle Radar Topography Mission (SRTM) data in ArcGIS 10.21. First, we made a mosaic using the individual DEM. The size of the filter reflects the wavelength of the smoothed topography. Progressive smoothing allows the removal of a high frequency and amplitude signal that contributes to masking any surface expression of the dynamically supported swell. For example, a 100 km filter removes all topographic features that have a wavelength that is <100 km and preserves all topographic features that are >100 km (Wegmann et al., 2007). The DEM was first resampled to a 50 m resolution in ArcMap. The neighborhood statistics tool was used to apply three low pass filters at variable λ to the dataset : 100 km, 200 km, and 250 km. A moving window, the size which corresponds to λ, was passed through the DEM and calculated mean elevation for the total number of pixels contained within λ, and the resulting mean values was re-plotted in each individual pixel.

Swath Profiles

Minimum, Mean, and Maximum elevation measurements were calculated from 30m DEM SRTM dataset. Swath profile width ranged from 80-120 km, and length ranges from Swath profiles allow extraction of mean elevation data which is useful for assessing longer wavelength topographic features and removes noise associated with shorter wavelength topography and high relief. Mean elevation permits first order observations of tectonic processes that support crustal elevation (Cassel et al., 20012; Coblentz et al., 2007).

Swath profiles were extracted from the SRTM dataset. The target swath area was outlined with a user-created polygon, and then, equal length line features were drawn parallel to the polygon with equal spacing between the lines. Swaths were between 75 and 100 km wide, and lines were drawn at 5 km intervals. Distance and elevation profiles were extracted for each individual line and inserted into a spreadsheet. Maximum, minimum, and mean elevations were extracted for each length segment with simple MS Excel functions (Figure…and…). This manual method of extracting swath profiles permitted us to extract a swath profile along the Snake River Plane/track of the Yellowstone Hot Spot (figure 3a), which does not follow a straight path.

Model

Braun et al (2013) published a model for predicting the first order surface expression of dynamic topography. A Gaussian function (eq 1) permits an approximation to topography forced by upwelling in a mantle plume with a head width of 2λ beneath a plate that moves at velocity v in x direction, where z_0 is the maximum expected amplitude of dynamic topography, and t is time.

Eq. 1 $z(x)=z_0e^{-(x-vt)^2/}\lambda^2$

The rates of uplift and subsidence as the plate passes over the plume head is described as:

Eq. 2 $z(x)=v\ dz/dx=2vz_0(x-vt)/\ \lambda^2\ {*}e^{-(x-vt)^2/}\lambda^2$

In MATLAB, we applied the best available estimated parameters for the Yellowstone plume, which has a width of 100 km (Smith et al, 2009) and a plate motion for North America over the plume head of 2.9 cm yr^{-1} (Pierce and Morgan, 2009) to these to equations to have a first order prediction of the uplift, subsidence and incision rates that could occur in the North American Plate as it passes over the Yellowstone plume.

Stream Profile Analysis

Observations from streams around the world on the relationship between local channel gradient (S) and contributing area (A) have allowed for analysis and interpretation of river profiles to understand landscape evolution forcing mechanisms (Wobus et al, 2006). When a stream is at equilibrium or grade, meaning, it is neither in an erosive or aggradational regime (Mackin, 1948), the slope of the channel can be expressed as:

$$\text{Eq. (3)} \quad S = k_s A^{-\theta}$$

Where k_s is a measure of channel steepness, or the 'channel steepness index' and θ is a measure of how the slope varies with changes in contributing drainage area, also known as the 'concavity index' (Rosenberg et al, 2013). Our analysis in TecDEM normalizes k_s to k_{sn} in order to compare streams with different drainage areas, because small variations in the concavity index can lead to large variations in the channel's slope. k_{sn} is calculated using a fixed reference θ of 0.45 (Snyder et al., 2000, Wobus et al., 2003; 2006). A stream profile that does not have a monotonical concave up profile expresses a transient disturbance (or convexity). Disturbances to graded profiles may result from lithological contrasts (Pederson, 2013), fault boundaries (Wobus et al, 2006; Kirby and Whipple, 2012), or climate control of discharge (Snyder, 2001).

Recent work suggests that stream profile analysis is useful in understanding differential rock uplift and permanent deformation of the crust in areas forced by long wavelength sub-lithospheric processes that have a low amplitude surface expression (Karlstrom et al (2012), Pederson et al (2013), and Rosenberg et al (2013)).

In this paper, we use stream profile analysis as a preliminary assessment tool of long wavelength deformation in waxing and waning regions of the proposed dynamic topography swell. In both cases, the streams should be out of equilibrium. We selected streams that are in regions predicted to be of incipient uplift to the east and north of YFV:

Greybull, North, and South Forks of the Shoshone river; We also selected streams in regions that are predicted to be actively subsiding, to the west and southwest of the YVF: Snake and Henrys Fork rivers. Stream data were extracted and analyzed with the Matlab-based TecDEM from 90m SRTM datasets (Shahazad and Gloaguen, 2012a; 2012b).

Slope/Area plots were extracted from the longitudinal stream profiles to MS Excel from Matlab. We calculated slope averages for every 10 kilometers along the longitudinal profile, and plotted the data in log/log space. This permitted us to remove the knickpoint created by the Buffalo Bill Dam and Reservoir system in the Shoshone River drainage. *Slope/Area plots for the Snake and Henrys fork River are on their way.*

Results

Swath Profile Results

The purpose of the swath profiles is to identify and assign the range of wavelengths attributable to various forcing mechanisms that have shaped the GY/SRP region. Mean elevation calculation is necessary to identify regionally extensive high elevation and limits confusion that arises from attributing high relief to high elevation (Burbank et al, 1997). The swath profiles aid in characterizing regional topographic features and relating them to other datasets. The three swath profiles that are presented here help describe long wavelength dynamic topography in three dimensions. The principal wavelengths of topography that we identified are: volcanic (<30 km wavelength, <1 km amplitude), non-glacial climate (<1 km wavelength, <0.5 km amplitude), glacial climate (<20 km wavelengh, <2 km amplitude), Basin and Range tectonic (< 50km wavelength, <2 km amplitude), Laramide tectonic (<200 km wavelength, <2.5 km amplitude), Dynamic topography signal (<800 km wavelength, <1.5 km amplitude).

The principal feature that all three profiles share is the Yellowstone Volcanic Field, which is represented by YVF in Fig 5. In A-A', the caldera is between km 690-710; in B-B' it is between km 380-400; and in C-C' is between km 260-and 300. The caldera is identifiable from by the comparatively lack of relief when it is compared to the area surrounding it. There are two clear examples in profile A-A' of the volcanic topographic signal, those are the Picabo and Heise Volcanic Fields (PVF and HVF, respectively). These are regions of no relief and all three show the distinctive caldera shape associated with the formation of these features.

The non-glacial climate topographic signal could be considered to be ‘noise’ in the overall topography signal. The low wavelength (<1 km) and low amplitude (0.5 km) does not seem to provide much variation throughout the swath profile when considering the full length of the swaths.

The glacial climate signal is clearly expressed in profiles A-A’. It has a wavelength of <20 km and an amplitude of <2 km. In A-A’, between km 790 and 810 displays a significant amount of relief (difference between minimum and maximum elevation), and showing the characteristic nearly horizontal profile associated with glaciated valley floors minimum elevation.

Basin and Range tectonic signal is detectable in profiles B-B’, between km 100 and 250; and C-C’, between km 0-200. Basin and range topography is characterized by graben and tilt block sequences that have a high mean elevation (+1 km).

The Laramide tectonic signal is in the 100-200 km wavelength and is identifiable in all three swath profiles. In A-A’, it is located between km 750 and 850, Beartooth mountains and between km 850-950 which is the Bighorn basin. In B-B’, the Beartooth mountains and Bighorn basin appear again, and however the evidence for this signal is strengthened by the inclusion of the Bighorn Bountains , that are between kms 600-680. In profile C-C’, the Laramide contribution to topography is preserved between km 375 and 550 in the form of the Wind river range and basin, this appears because the swath was taken parallel to the NW-SE trend of the range and basin, meaning that this is the longest possible signal for a Laramide contribution to topography.

In all three profiles there is a broad regional high mean elevation swell, there are few places where the mean elevation is <1 km. We interpret the broad high mean elevations in all three swaths to correspond the long wavelength topography.

Topographic Filtering Results

Identifying the multiple wavelengths of topography preserved in the GY/SRP region permits us to determine the size of the filter to be applied to SRTM dataset. By filtering all wavelengths <200 km allows for a reasonable identification of long wavelength topography (citation…). We present results of progressive filtering from 50-250 km in

Fig 4. Each figure includes progressive removal of shorter wavelength topography, revealing an asymmetric distribution of elevation that matches the shape of A-A' profile, suggesting that the shape of the swell in north America is comparable to that of a wave.

Modeling Results

Parameterization of Braun et al.'s (2013) model of advection of a topographic swell with best available estimates/data for the Yellowstone plume (Smith et al., 2009; Humphreys et al., 2000). Plate velocity, v, is 2.9 cm/yr (Pierce and Morgan, 1992), the maximum displacement is 0.5 km (Smith et al., 2009), and the plume half-width is 100 km (Smith et al. 2009). Line colors correspond to time. Dashed lines correspond to tectonic features, WBB – Western Bighorn Basin, CBB – Central Bighorn Basin. Model replicates position of the topographic swell at 10.3 Ma (Picabo) and shows migration of the swell to its present at the Yellowstone caldera (0.64 Ma). The model makes predictions for rate of uplift/subsidence based on the advection rate of the swell. The model predicts that there should be differential uplift in the space that separates the western edge of the Bighorn Basin (WBB) from the central Bighorn Basin (CBB), and the eastern edge of the basin (EBB, not shown). These are regions that are on the periphery of the predicted zone of influence of the Yellowstone dynamic topography.

Stream Profile Analysis Results

Results from stream profile analysis for selected streams in areas inferred to be under the influence of the Yellowstone swell are presented. Streams in the waxing topography are the Greybull North Fork and South Fork Shoshone. Streams in the waning topography are the Henrys Fork and Falls River.

The profile of the Greybull river, figure 7C contains two significant knickpoints. Once at Km 20 and one at Km 100. The 20km knickpoint corresponds a glacial cirque in the upper reaches of the drainage. The knickpoint at km 100 does not correspond to any other feature that has been identified by DEM, topographic, or geologic maps. There are four distinct breaks in slope that are identifiable in figure 7f, the first one corresponds to the upstream cirque, the second to the previously mentioned unidentified profile convexity, the third, which is the largest break in slope corresponds to the bedrock-alluvial transition, and the final break in slope corresponds to the confluence with the Bighorn River near the town of Greybull.

I am still working on getting Ksn and the rest of the results from the stream profile analysis values for all streams… main point for results is referring to the various profiles and commenting on the shape of the streams in the leading edge of the dynamic topography (incipient uplift) and the two streams in the subsiding part of the stream.

Discussion

Points to be included in discussion section:

- Climate contribution to landscape evolution in this region (Riihimaki et al, 2007).
- Relationship between topography and mantle p-wave datasets.
- Recent geophysical modeling (Becker et al, 2013)… Update on Lowry et al model with Earthscope data.
- Previous studies have focused efforts in regions of high relief, advantages and disadvantages of doing this.
- Going to regions of low relief to use geomorphic markers to measure dynamic topography.
- The challenge of identifying vertical (amplitude) signal from these methods.

Conclusions

- There is a clear correlation between mantle temperature and mean elevation in the GY/SRP region, with highest temperature (slowest V_p).
- Coincidence of highest geoid anomaly values in Western North America centered in the Greater Yellowstone Area with the high relief Laramide and Absaroka ranges indicates deep mantle support for the region.
- Filtered topography reveals topographic swell with steep gradient to the northeast and less steep to the southwest, which is consistent with swath profile, temperature gradient, and model results.
- Stream profile analysis reveals steepening of streams in the waxing topography and aggradation in the waning topography as the plate passes over the uplift source.
- Analysis reveals that region of influence of topographic swell extends beyond the YCHT and into adjacent Yellowstone and Bighorn basins.

- Model makes predictions for advection of a swell that should have an uplift (erosion signal) and subsidence (aggradation signal) as a plate passes over the plume uplift source.
- Laramide blocks, Eocene volcanics, and Basin and Range extensional features, and caldera volcanism that are a part of the region of high relief (YCHT) mask any signal of dynamic topography, even though this region incorporates the signal into its complex topography.
- The bighorn basin and Yellowstone river basins are areas of low relief with a clear Quaternary erosional history and they are ideal for detecting the surface expression of the Yellowstone hotspot.

Figure Captions

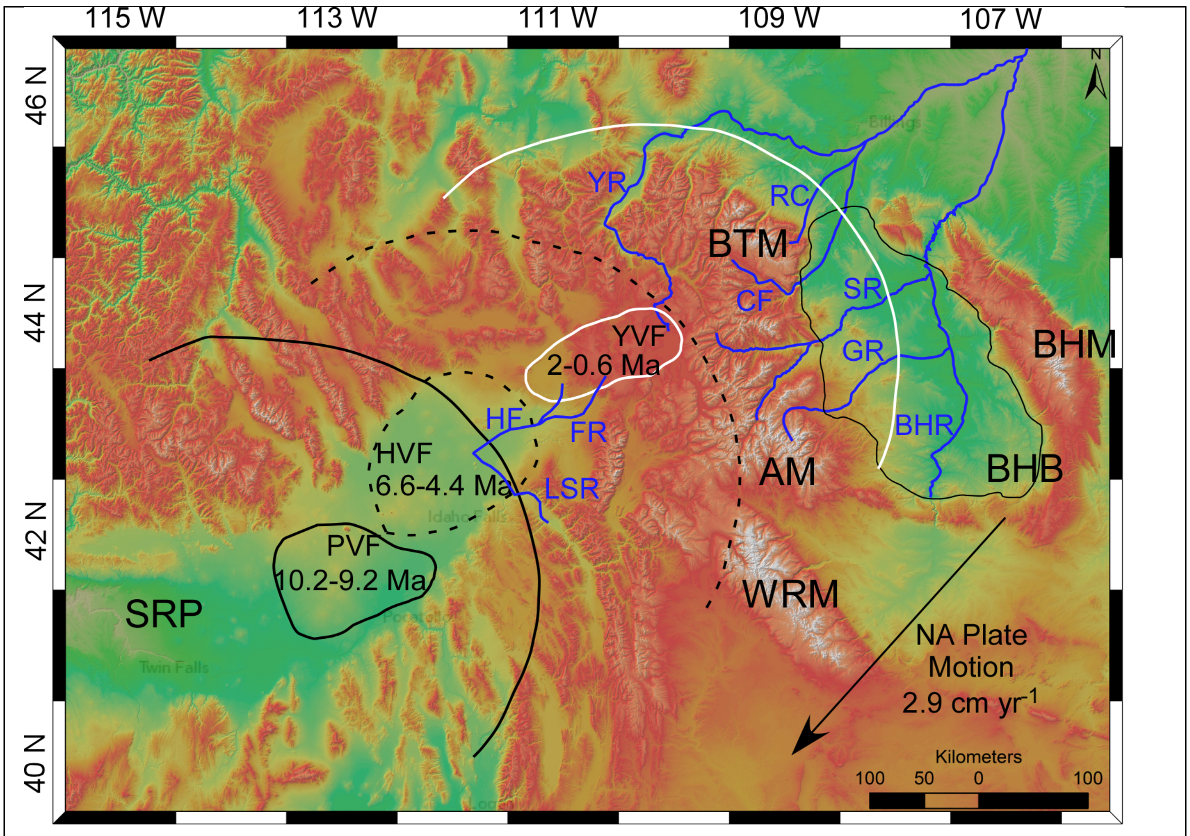

Figure 1. Shaded Relief Location Map showing Swell.

Shaded relief DEM showing area of study. Regional map of the Greater Yellowstone area. Individual volcanic centers associated with the hotspot: Picabo (black - PVF; 10.2-9.2 Ma), Heise (black dash - HVF; 6.6-4.4 Ma), and Yellowstone (white - YVF; 2-0.6 Ma). Crescent shaped curves represents the inferred minimum extent of topographic swell associated with an individual volcanic center (Smith et al, 2009). White polygon is the area covered by swath profile (Fig. 2). Blue abreviations correspond to major streams in the study area: YR- Yellowstone, CF- Clarks Fork of the Yellowstone, SR- Shoshone, GR- Greybull, BHR- Bighorn River, SR-Snake River, HF-Henry's Fork. Includes major physiographic features of the region: Bighorn Basin (BHB), Beartooth Mountains (BTM), Absaroka Mountains (AM), Wind River Mountains (WRM), Bighorn Mountains (BHM), Snake River Plain (SRP). Highlighted rivers are those associated with this study: Bighorn, Greybull, Shoshone, Clarks Fork, Rock Creek, and Yellowstone.

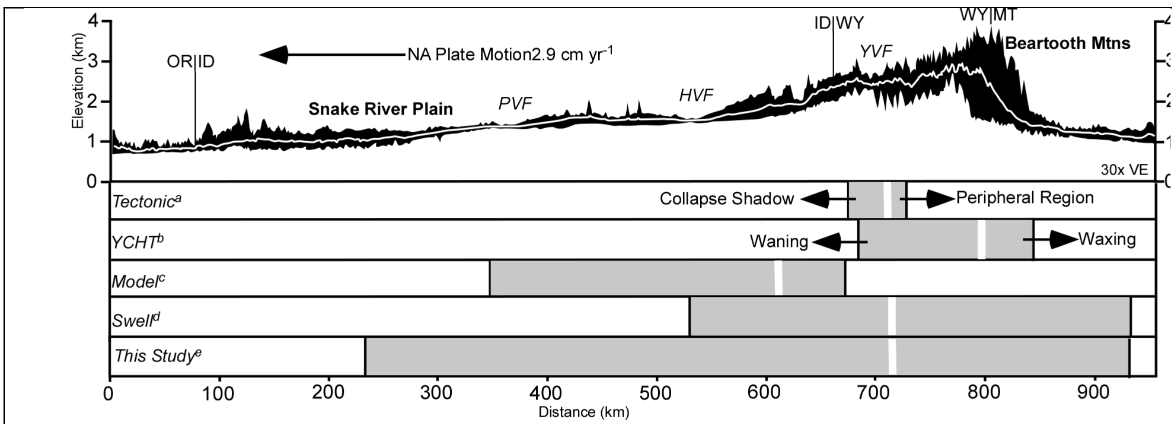

Figure 2. Swath Profile with different models. Profile with maximum, mean, and minimum elevations for a 80 km-wide swath taken along the Snake River Plain, following the track of the Yellowstone hotspot (Pierce and Morgan, 1992), from Oregon/Idaho border (OR|ID), Idaho/Wyoming border (ID|WY), and Wyoming/Montana border (WY|MT). Includes motion vector for North America. Shows location of Picabo (PVF), Heise (HVF), and Yellowstone (YVF) Volcanic Fields. Includes four interpretation of the non-volcanic expression of the Yellowstone hotspot: Tectonic[a]- Tectonic Parabola of Anders et al (1989), Yellowstone VF is the apex of a parabolic region of concentrated seismicity, Peripheral region is the area on the outer edge of the Tectonic Parabola, and collapse shadow is the area that has already been affected by seismicity, Snake River Plain. YCHT[b]- Pierce and Morgan's (1992) Yellowstone Crescent of High Terrain, with Waxing topography ahead of the motion of the swell and waning topography after the terrain has passed over the uplift source. Model[c]- Lowry et

al (2000) model results predicted that the region that would be influenced by dynamic topography. Swell[d]- Smith et al. (2009) proposed a symmetrical swell with its apex centered on the YVF. In each interpretation, the gray shaded area represents the extent of the surface expression of the hotspot and the white band represents the apex of each expression. This study[e]- Results from analysis and data integration lead us to present our assessment for Yellowstone dynamic topography.

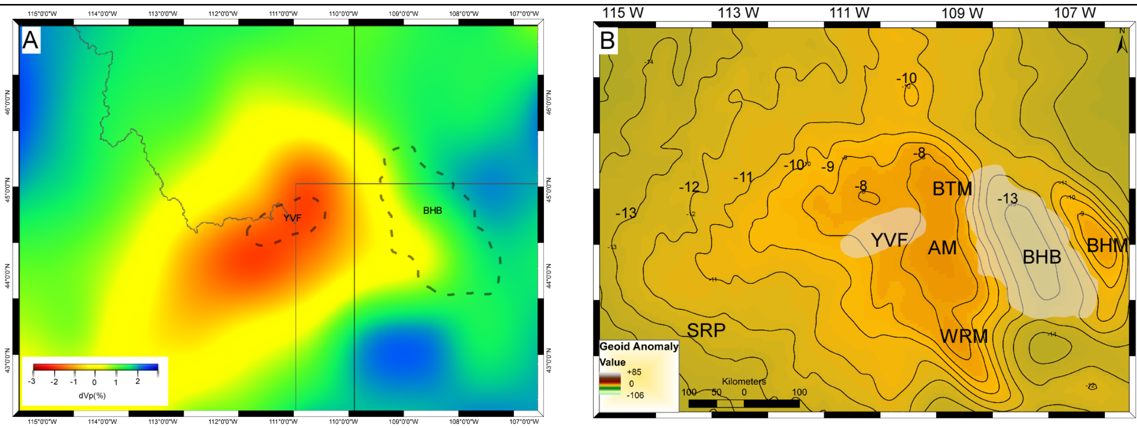

Figure 3. **Geoid Anomaly and mantle % V_p disturbance map** Geoid anomaly map of the greater Yellowstone region, extracted from the Earth Gravitational Model (2008). Values range from -15m to -8 throughout the study area. Anomaly values for the Yellowstone Volcanic Field (YVF) are between -9 and -8m. Highest geoid anomalies coincide with the Beartooth, Absaroka, Wind River and Bighorn mountains. Sharp decrease in geoid anomaly values between Absaroka and Bighorn mountains coincides with the Bighorn Basin (BHB). High topography supported by deep mantle processes.

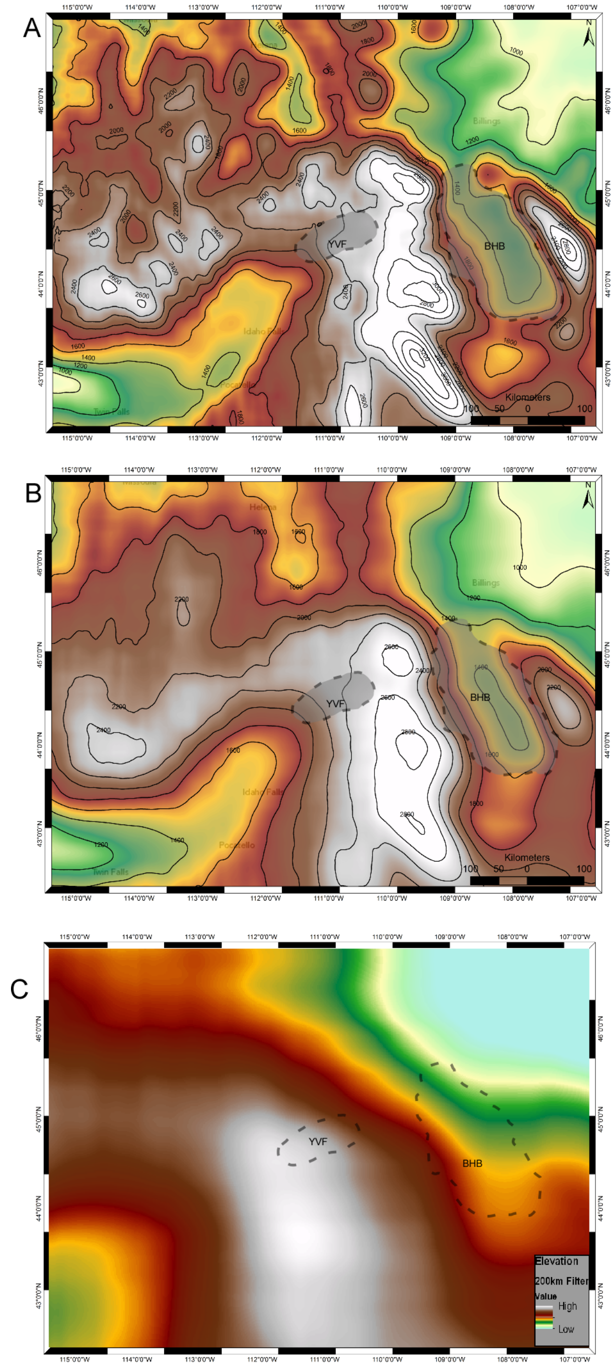

Figure 4. Filtered Topography Results of low-pass filtering on SRTM data of the Greater Yellowstone/Snake River Plain, progressive smoothing identifies longer wavelength topographic features. A. 50 km filter. B. 150 km filter. C. 250 km filter. The purpose of the topographic filtering to parse variable wavelengths of the multiple forcing signals preserved in the GY/SRP region.

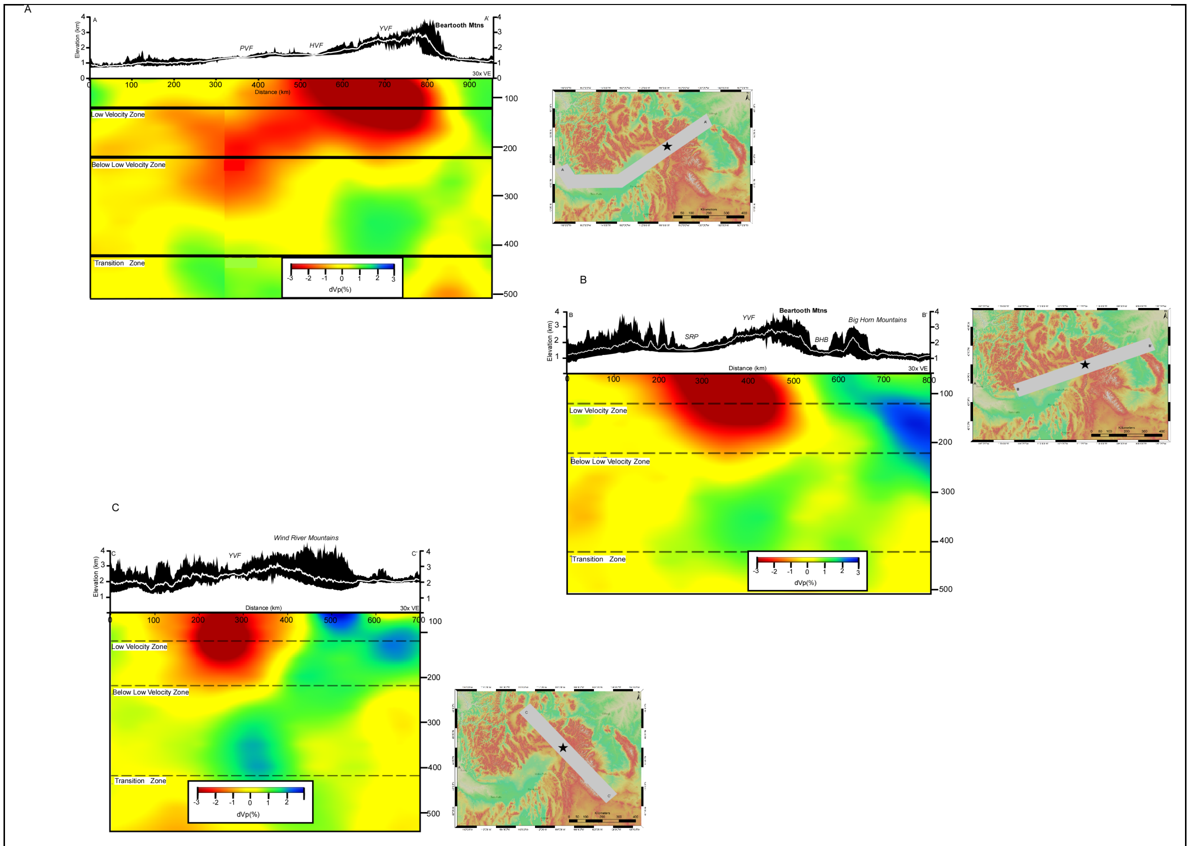

Figure 5. Swath Profiles with p-wave data Swath profiles that cross the Yellowstone Volcanic Field (YVF, star) from different directions. A-A': profile along the hot spot track/ snake river plain. B-B': SouthWest –NorthEast, includes northern Bighorn Basin. C-C': NW-SE: Includes Madison and Gallatin in the Northwest, and the Wind River Mountains and Basin in the Southeast.

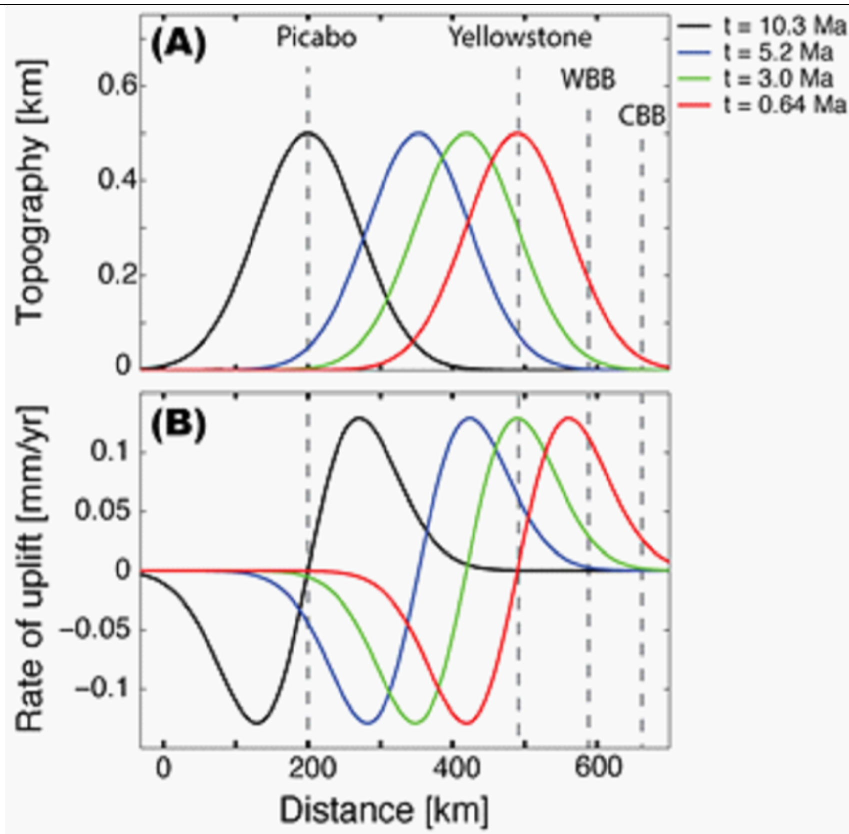

Figure 6. The Braun et al. (2013) analytical solution provides a first order approximation of the effect of dynamic topography on the resultant uplift rate (Fig. 5). Braun et al. begin with a Gaussian function for the topographic uplift due to passing a plate over a plume as a function of plume width, plate velocity and time. Our preliminary application of this model reveals that predicted uplift and uplift rates yield a spatially resolvable pattern in a model North American plate as it passes over the Yellowstone hotspot.

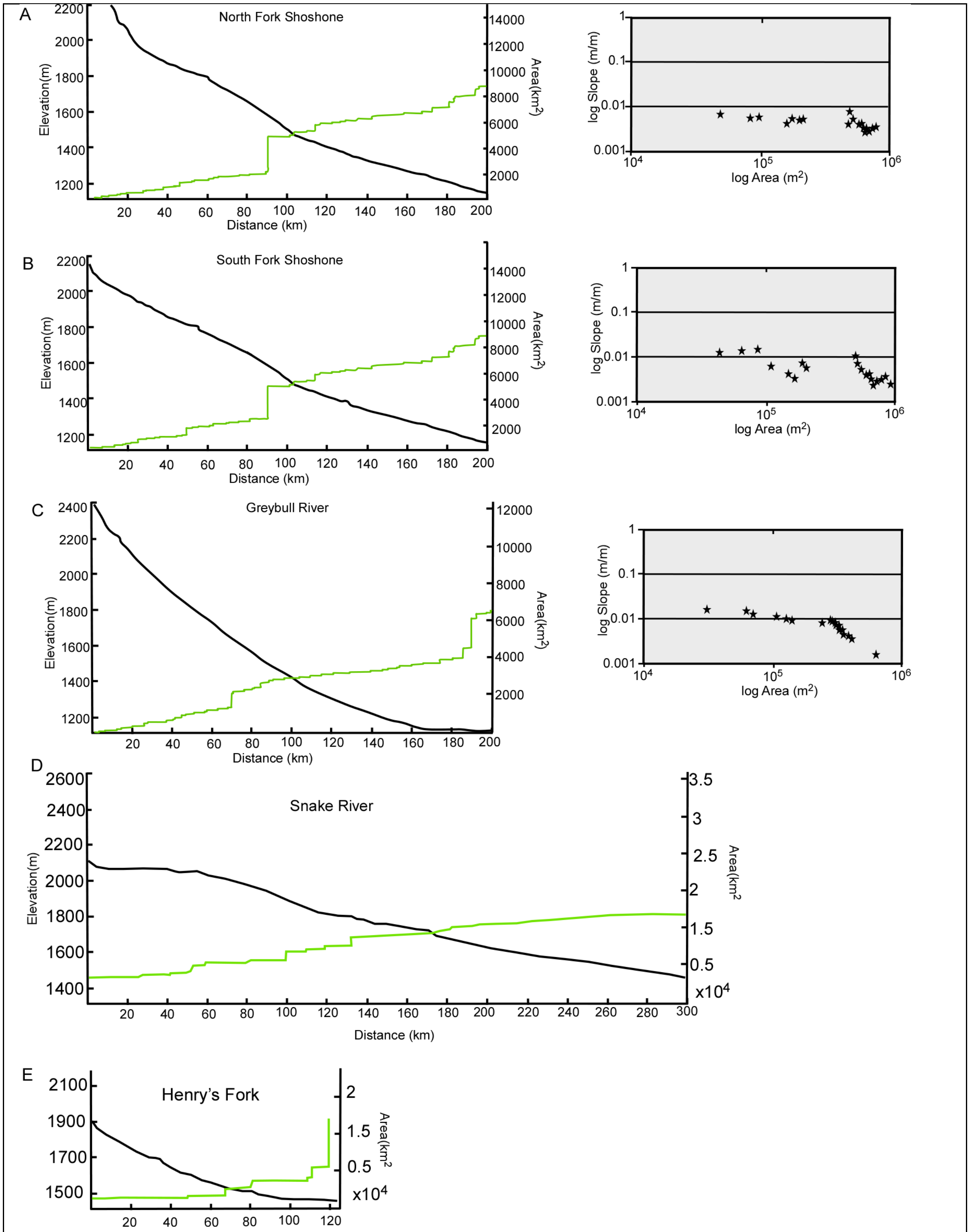

Figure 7. Stream profiles, slope/area plots and map showing stream location for: Greybull, North and South fork Shoshone, Snake and Henry's Fork Rivers. The Greybull, and Shoshone rivers are in the region inferred to be ahead of the wave of

dynamic topography, and the Snake and Henry’s Fork rivers are in the area predicted to be subsiding behind the wave of topography after passing the uplift source.